Change in the Mode of Inhibition of Acetylcholinesterase by (4-Nitrophenyl)sulfonoxyl Derivatives of Conformationally Constrained Choline Analogues

Prashant S. Savle,[†] Rohit A. Medhekar,[‡] Ella L. Kelley,[‡,§] Jerome G. May,[⊥] Steven F. Watkins,[⊥] Frank R. Fronczek,[⊥] Daniel M. Quinn,[‡] and Richard D. Gandour*,[†]

Department of Chemistry, Virginia Tech, Blacksburg, Virginia 24061-0212, Department of Chemistry, The University of Iowa, Iowa City, Iowa 52242, Department of Chemistry, Southern University, Baton Rouge, Louisiana 70813, and Department of Chemistry, Louisiana State University, Baton Rouge, Louisiana 70803-1804

Received February 10, 1997[⊗]

A chiral, five-step synthesis of 2-(hydroxymethyl)-2,4-dimethylmorpholine (**12**) from (*R*)- and (*S*)-2-methylglycidols gives an overall yield of 63%. Morpholines (*R*)- and (*S*)-**12** are converted into 2-(azidomethyl)-2,4-dimethylmorpholine (**15**) via 2,4-dimethyl-2-[[(4-nitrophenyl)sulfonoxy]-methyl]morpholine (**14**). The tertiary morpholines **12**, **14**, and **15** are quaternarized to afford 2-(hydroxymethyl)-2,4,4-trimethylmorpholinum iodide (**2**), 2,4,4-trimethyl-2-[[(4-nitrophenyl)-sulfonoxy]methyl]morpholinium iodide (**3**), and 2-(azidomethyl)-2,4,4-trimethylmorpholinium iodide (**4**), respectively, which all inhibit acetylcholinesterase (AChE). These morpholinium inhibitors are compared with conformationally constrained aryl hemicholinium AChE inhibitors. Enantiomers of **2** and **4** are reversible competitive inhibitors of AChE, with values of $K_i = 360 \pm 30$ μM for (*S*)-**2**, 650 ± 90 μM for (*R*)-**2**, 450 ± 70 μM for (*S*)-**4**, and 560 ± 30 μM for (*R*)-**4**, respectively. Enantiomers of **3** are noncompetitive inhibitors of AChE with values of $K_i = 19.0 \pm 0.9$ μM for (*S*)-**3** and 50 ± 2 μM for (*R*)-**3**, respectively. AChE shows a 2-fold chiral discrimination in the case of inhibition by **2** and **3**. Inhibition also changes from competitive to noncompetitive when (3-hydroxyphenyl)-*N*,*N*,*N*-trimethylammonium iodide (**18**) [$K_i = 0.21 \pm 0.06$ μM; Lee, B. H., Stelly, T. C., Colucci, W. J., Garcia, J. G., Gandour, R. D., and Quinn, D. M. (1992) *Chem. Res. Toxicol.* **5**, 411−418] is converted into [3-[(4-nitrophenyl)sulfonoxy]-phenyl]-*N*,*N*,*N*-trimethylammonium iodide (**5**), $K_i = 6.0 \pm 0.5$ μM. These results indicate that the 4-nitrobenzenesulfonyl group controls the mode of inhibition.

Introduction

Acetylcholinesterase (AChE)[1] mediates the chemical transmission of nerve impulses in the body. AChE, a serine esterase, catalyzes the hydrolysis of the neurotransmitter acetylcholine by a well-precedented acyl enzyme mechanism (*1*, *2*). Inhibitors of AChE serve

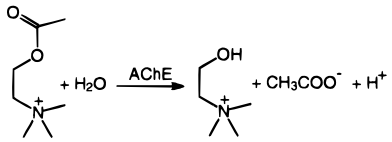

many roles in mental wellness, pest control, and chemical warfare. Designing AChE inhibitors dates back to Stedman (*3*) in 1929, and many types of inhibitors abound (*2*). Some of the strongest *reversible* inhibitors bind to two sites on the enzyme, the active site and a peripheral site (*2*, *4*). Inhibitors that bind only in the active site show competitive inhibition, while those that bind only in the peripheral site show noncompetitive inhibition.

The X-ray crystal structure of *Torpedo californica* AChE reveals an active site, that possesses a hydrogen-bonded catalytic triad, consisting of Ser200, His440, and Glu327, which is located at the bottom of a deep and narrow gorge (*5*). As in the serine proteases, Ser200 and His440 function as nucleophilic and general base catalysis, respectively (*2*, *6*). The active site of AChE accommodates a wide range of ligands (*6*). Photoaffinity labeling studies assign Trp279 to the peripheral site, which is located ∼14 Å from the active site. The peripheral site recognizes quaternary ammonium ions that inhibit enzymatic activity (*7*). X-ray structures of bisquaternary compounds bound to AChE show ligands binding at the peripheral site by interaction with the π-electrons of the Trp279.

Racemic hemicholinium compounds **1** inhibit AChE (*8*). Hemicholiniums exist in open and cyclic forms (*9*), although the equilibrium favors the cyclic morpholinium structure with the hydroxyl group axial and the R group equatorial. Morpholiniums provide a conformationally constrained molecular skeleton on which to anchor other groups to explore the stereochemical topography of the active site. Nonracemic 2,2-disubstituted *N*,*N*-dimeth-

[†] Virginia Tech.
[‡] The University of Iowa.
[§] Southern University.
[⊥] Louisiana State University.
[⊗] Abstract published in *Advance ACS Abstracts,* December 1, 1997.
[1] Abbreviations: AChE, acetylcholinesterase; DTNB, 5,5′-dithiobis-(2-nitrobenzoic acid); TBDMS-Cl, *tert*-butyldimethylsilyl chloride; DMAP, 4-(dimethylamino)pyridine; KH, potassium hydride; TBAF, tetrabutylammonium fluoride; MTPA, α-methoxy-α-(trifluoromethyl)phenylacetic acid; DCC, 1,3-dicyclohexylcarbodiimide.

S0893-228x(97)00019-2 CCC: $15.00
Published on Web 01/19/1998

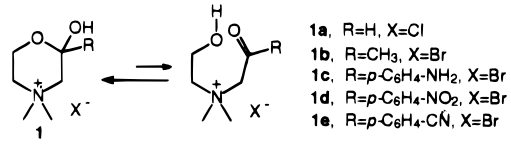

1

ylmorpholinium compounds **2**−**4** suit our goal for exploration as the individual enantiomers can be synthesized.

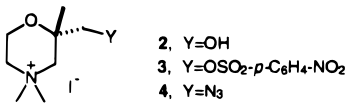

Initial Rationale. We based our choice for examining enantiomers **2**−**4** as AChE inhibitors on various ideas. We envisioned that the hydroxyl group in **2** could form hydrogen bonds to His440 and the enantiomers could show strong stereoselectivity. We thought that the azido group in **4** could potentially serve as a photolabeling group to show where the enantiomers bound in the active site. We decided to assay **3** because we could make it readily, and we could rationalize that the sulfonoxyl group in **3** could serve as a transition-state analogue with the nitrophenyl ring interacting strongly with the walls of the gorge leading to the active site. As with many cases in research, our initial rationale for assaying **2** and **4** produced modest results. To our delight, assays of **3** produced a discovery.

In this report, we describe the chiral syntheses and structures of the *R* and *S* enantiomers of **2**−**4** and the inhibition of AChE-catalyzed hydrolysis of acetylthiocholine by them. The stereoisomers of **2** and **4** show competitive inhibition, while those of **3** show noncompetitive inhibition. We also describe the noncompetitive inhibition by [3-[(4-nitrophenyl)sulfonoxy]phenyl]-*N*,*N*,*N*-trimethylammonium iodide, **5**.

Synthesis. Interest is increasing in the 2-morpholinylmethyl group for its neuropharmacological and gastrokinetic properties (*10*, *11*). There are no reports on the synthesis of nonracemic 2,2-disubstituted morpholines, only chiral syntheses of 2-substituted, 2,6-disubstituted (*12*), and 2,3,6- (*13*), 2,2,6- (*14*), and 2,5,5- (*15*) trisubstituted analogues, which are unsuitable for preparing **2**−**4**. 2-Substituted morpholine is synthesized by opening nonracemic benzyl glycidyl ether with 2-aminoethylhydrogen sulfate and then cyclization with sodium hydroxide to give the morpholine in 37−55% yield (*10*, *11*). This protocol in our hands, however, fails to produce any 2,2-disubstituted morpholine from benzyl 2-methylglycidyl ether, because side products form more rapidly than the desired product. A three-step approach, opening a protected 2-methylglycidol with *N*-methylaminoethanol followed by transformation of the unprotected primary alcohol into a leaving group and then intramolecular nucleophilic substitution, gives the desired 2,2-disubstituted morpholine.

Experimental Procedures

General Methods. Uncorrected melting points were measured on a digital melting point apparatus equipped with multistage ramping rates from 0.1 to 10.0 °C/min. ^{1}H NMR spectra were recorded at 200, 270, and 400 MHz. ^{13}C NMR spectra were recorded at 100 MHz. Unless noted otherwise, all NMR spectra were recorded in $CDCl_3$. Proton chemical shifts are expressed in ppm downfield from internal TMS. Coupling constants (expressed as J_{app} in Hz) were the observed separation between the lines. ^{13}C chemical shifts are also expressed in ppm relative to the solvent chemical shift. Assignments of the ^{1}H and ^{13}C NMR signals were made by comparison with similar compounds and using 2D ^{13}C−^{1}H correlation and 2D ^{1}H COSY experiments. Infrared spectra, reported in cm^{-1}, were recorded as thin films on KBr cells. FAB MS samples were prepared by suspending in glycerol. Elemental analyses were performed by Atlantic Microlabs of Norcross, GA. The optical rotations were recorded in a 10- × 100-mm cell.

Unless otherwise noted, materials were obtained from commercial sources and used without further purification. THF was distilled from sodium−benzophenone ketyl. Diethyl ether was distilled from sodium. Triethylamine and nitromethane were distilled from CaH_2 and stored over Linde molecular sieves type 3 Å. CH_2Cl_2 was distilled over CaH_2. MeOH was distilled over a small amount of Mg. Solutions were dried over $MgSO_4$ and concentrated by rotary evaporation, unless specified otherwise.

(*R*)-1-[[(*tert*-Butyldimethylsilyl)oxy]methyl]-1-methyloxirane, (*R*)-7 (*16*). To a stirred solution of (*S*)-2-methylglycidol (5.6 g, 63 mmol) and anhydrous NEt_3 (7.1 g, 70 mmol) in dry CH_2Cl_2 (50 mL) was added a solution of *tert*-butyldimethylsilyl chloride (TBDMS-Cl) (10.1 g, 66.8 mmol) in dry CH_2Cl_2 (20 mL) dropwise at room temperature. After stirring for 4 h at room temperature, the cloudy solution was filtered through Celite. The filtrate was washed with saturated $NaHCO_3$ solution (1 × 20 mL) and brine (1 × 25 mL). The organic phase was dried and concentrated. The residue was purified by flash chromatography (5% EtOAc−hexanes) to afford 12.7 g (98%) of (*R*)-**7** as a colorless oil. TLC R_f = 0.2 (15% ether−hexanes, silica). ^{1}H NMR (400 MHz): 0.06 (s, 3H), 0.07 (s, 3H), 0.89 (s, 9H), 1.34 (s, 3H), 2.59 (d, J_{app} = 5.2 Hz, 1H), 2.75 (d, J_{app} = 4.8 Hz, 1H), 3.60 (d, J_{app} = 11.2 Hz, 1H), 3.65 (d, J_{app} = 11.2 Hz, 1H). ^{13}C NMR (100 MHz): −5.5, 17.9, 18.2, 25.8, 51.4, 56.9, 66.5. IR (neat): 1102, 1462, 3048. Anal. Calcd for $C_{10}H_{22}O_2Si$: C, 59.37; H,10.97. Found: C, 59.31; H, 10.92. $[\alpha]^{23}_D$ −3.7° (*c* 5.8, $CHCl_3$).

Data for (*S*)-7: found C, 59.48; H, 11.12. $[\alpha]^{23}_D$ +3.8° (*c* 2.3, $CHCl_3$).

(*R*)-[3-[(*tert*-Butyldimethylsilyl)oxy]-2-hydroxy-2-methylpropyl](2-hydroxyethyl)methylamine, (*R*)-8. A solution of (*R*)-**7** (3.7 g, 18.4 mmol) and 2-(methylamino)ethanol (1.4 g, 18.4 mmol) in MeOH (60 mL) was stirred for 12 h at 50 °C. The reaction mixture was concentrated to yield a pale yellow residue, which was purified by column chromatography on neutral alumina, eluting with 5% MeOH−EtOAc to give (*R*)-**8** as a colorless oil, 4.4 g (87%). TLC R_f = 0.3 (10% MeOH−EtOAc, neutral alumina). ^{1}H NMR (270 MHz): 0.06 (s, 6H), 0.9 (s, 9H), 1.13 (s, 3H), 2.37 (d, J_{app} = 14 Hz, 1H), 2.39 (s, 3H), 2.56 (d, J_{app} = 14 Hz, 1H), 2.64−2.67 (m, 2H), 2.8 (br, 1H), 3.44 (br s, 2H), 3.61 (t, J_{app} = 5.2 Hz, 2H). ^{13}C NMR (100 MHz): −5.5, 18.2, 22.9, 25.8, 45.1, 59.6, 61.5, 63.5, 68.3, 72.9. IR (neat): 3458. MS *m*/*z* (CI): 278 (M^+ + 1), 246 (M^+ − CH_3OH), 220 (M^+ − *tert*-C_4H_9). Anal. Calcd for $C_{13}H_{31}O_3NSi$: C, 56.28; H,11.27; N, 5.05. Found: C, 56.12; H, 11.21; N, 4.98. $[\alpha]^{23}_D$ −0.44° (*c* 4.1, $CHCl_3$).

Data for (*S*)-8: found C, 56.20; H, 11.14; N, 4.94. $[\alpha]^{23}_D$ +0.40° (*c* 2.1, $CHCl_3$).

(*R*)-[3-[(*tert*-Butyldimethylsilyl)oxy]-2-hydroxy-2-methylpropyl](2-chloroethyl)methylamine, (*R*)-9. To a solution of (*R*)-**8** (2.01 g, 7.02 mmol) and NEt_3 (1.8 g, 18.1 mmol) in dry CH_2Cl_2 (10 mL) at room temperature was added tosyl chloride (TsCl) (1.5 g, 7.7 mmol) in dry CH_2Cl_2 (10 mL) dropwise in 30 min. The reaction mixture was stirred for 5 h and then diluted with CH_2Cl_2 (20 mL). The solution was washed with saturated $NaHCO_3$ (1 × 20 mL) and brine (1 × 25 mL). The extract was dried and concentrated to afford a dark brown oil, which was chromatographed on neutral alumina eluting with 1:1 hexanes−EtOAc to afford (*R*)-**9** as a pale yellow oil (1.8 g, 89%). TLC R_f = 0.35 (1:3 hexanes−EtOAc, neutral alumina). ^{1}H NMR (270 MHz): 0.04 (s, 6H), 0.89 (s, 9H), 1.09 (s, 3H), 2.26 (d, J_{app} = 13.8 Hz, 1H), 2.39 (s, 3H), 2.62 (d, J_{app} = 13.8 Hz, 1H), 2.79−2.85 (m, 2H), 3.0 (br s, 1H), 3.36 (d, J_{app} = 9.5 Hz, 1H), 3.42 (d,

J_{app} = 9.5 Hz, 1H), 3.54 (t, J_{app} = 6.6 Hz, 2H). ^{13}C NMR (67.5 MHz): −5.5, 18.1, 22.9, 25.8, 42.1, 44.6, 61.2, 63.4, 68.1, 72.1. IR (CH_2Cl_2): 3385. MS *m*/*z* (CI): 296 ($M^+ + 1$), 260 ($M^+ + 1 -$ Cl), 238 ($M^+ -$ *tert*-C_4H_9). Anal. Calcd for $C_{13}H_{30}O_2NClSi$: C, 52.85; H, 10.24; N, 4.74. Found: C, 52.81; H, 10.19; N, 4.65. $[\alpha]^{23}_D$ −7.3° (*c* 1, $CHCl_3$).

Data for (*S*)-9: found C, 52.61; H, 10.04; N, 4.61. $[\alpha]^{23}_D$ +7.1° (*c* 0.5, $CHCl_3$).

(*R*)-[3-[(*tert*-Butyldimethylsilyl)oxy]-2-hydroxy-2-methylpropyl][2-[[(4-methylphenyl)sulfonyl]oxy]ethyl]-methylamine, (*R*)-10. To a solution of (*R*)-**8** (2.01 g, 7.02 mmol), 4-(dimethylamino)pyridine (DMAP) (0.040 g, 0.31 mmol), and NEt_3 (1.82 g, 18.1 mmol) in dry CH_2Cl_2 (10 mL) at room temperature was added TsCl (1.5 g, 7.7 mmol) in dry CH_2Cl_2 (10 mL) dropwise in 30 min. The reaction mixture was stirred for 5 h and then diluted with CH_2Cl_2 (20 mL). The solution was washed with saturated $NaHCO_3$ (1 × 20 mL) and brine (1 × 25 mL). The extract was dried and concentrated to afford a dark brown oil, which was used without purification for the cyclization. Attempts to purify the crude tosylate by chromatography resulted in cyclization to morpholine as seen from the NMR. ^{1}H NMR (crude, 400 MHz): 0.04 (s, 6H), 0.89 (s, 9H), 1.1 (s, 3H), 2.26 (d, J_{app} = 13.8 Hz, 1H), 2.39 (s, 3H), 2.62 (d, J_{app} = 13.8 Hz, 1H), 2.79−2.85 (m, 2H), 2.8 (s, 3H), 3.0 (br s, 1H), 3.42 (d, J_{app} = 9.5 Hz, 1H), 3.64 (d, J_{app} = 9.5 Hz, 1H), 4.2 (t, J_{app} = 6.6 Hz, 2H), 7.35 (d, J_{app} = 9.1 Hz, 2H), 7.65 (d, J_{app} = 9.1 Hz, 2H). ^{13}C NMR (crude, 100 MHz): −5.5, 18.1, 20.1, 23.9, 25.8, 44.8, 56.9, 61.2, 63.4, 68.1, 71.8, 127.3, 129.7, 134.7, 143.5.

(*R*)-2-[[(*tert*-Butyldimethylsilyl)oxy]methyl]-2,4-dimethylmorpholine, (*R*)-11. A solution of (*R*)-**9** (2.1 g, 7.2 mmol) in dry THF (30 mL) was treated with potassium hydride (KH) (0.46 g, 1.32 g of 35 wt % mineral oil dispersion, 12 mmol) for 3 h. THF was removed under reduced pressure, and the dark reddish brown residue was dissolved in EtOAc (40 mL). The solution was washed with saturated $NaHCO_3$ (1 × 20 mL) and brine (1 × 25 mL). The extract was dried and concentrated to afford a red-dark brown oil, which was chromatographed on neutral alumina eluting with 9:1 hexanes−EtOAc to afford (*R*)-**11** as a colorless oil (1.8 g, 92%). TLC R_f = 0.15 (95:5 hexanes−EtOAc, neutral alumina). ^{1}H NMR (400 MHz): 0.05 (s, 6H), 0.89 (s, 9H), 1.23 (s, 3H), 2.17 (d, J_{app} = 10.8 Hz, 1H), 2.22 (s, 3H), 2.27 (d, J_{app} = 11 Hz, 1H), 2.25−2.29 (m, 1H), 2.33−2.39 (m, 1H), 3.49 (d, J_{app} = 9.2 Hz, 1H), 3.63 (d, J_{app} = 9.2 Hz, 1H), 3.69−3.81 (m, 2H). ^{13}C NMR (100 MHz): −5.4, 20.5, 22.9, 25.9, 46.7, 55.5, 61.4, 61.5, 67.4, 73.7. IR (neat): 1164, 1461, 1623. MS *m*/*z* (EI): 259 (M^+), 202 ($M^+ -$ *tert*-C_4H_9). Anal. Calcd for $C_{13}H_{29}O_2NSi$: C, 56.69; H, 10.62; N, 5.09. Found: C, 56.74; H, 10.49; N, 4.90. $[\alpha]^{23}_D$ −2.3° (*c* 0.1, $CHCl_3$).

Data for (*S*)-11: found C, 56.81; H, 10.55; N, 4.96. $[\alpha]^{23}_D$ +2.2° (*c* 0.21, $CHCl_3$).

(*R*)-2-(Hydroxymethyl)-2,4-dimethylmorpholine, (*R*)-12. A solution of (*R*)-**11** (3.0 g, 11 mmol) in THF (10 mL) was treated with solid $Bu_4N^+F^-$ (TBAF) (4.5 g, 17.3 mmol) for 8 h at room temperature. THF was carefully removed under reduced pressure, and the residue was purified on neutral alumina eluting with CH_2Cl_2 to yield (*R*)-**12** as a colorless volatile liquid (1.6 g, 91%). Bp: 102−104 °C. TLC R_f = 0.2 (1:3 hexanes−EtOAc, neutral alumina). ^{1}H NMR (400 MHz): 1.26 (s, 3H), 2.22 (d, J_{app} = 11.6 Hz, 1H), 2.24 (s, 3H), 2.31−2.42 (m, 2H), 2.53 (d, J_{app} = 11.6 Hz, 1H), 3.59 (d, J_{app} = 11.2 Hz, 1H), 3.74 (d, J_{app} = 11.2 Hz, 1H), 3.78−3.83 (m, 1H), 3.94−4.01 (m, 1H). ^{13}C NMR (100 MHz): 21.5, 46.4, 54.9, 61.5, 62.1, 68.3, 73.0. IR (CH_2Cl_2): 3358. MS *m*/*z* (EI): 145 (M^+). HRMS: calcd for $C_7H_{15}O_2N_1$ 145.1103, found 145.1102. $[\alpha]^{23}_D$ −2.9° (*c* 1.1, $CHCl_3$).

Data for (*S*)-12: HRMS calcd for $C_7H_{15}O_2N_1$ 145.1103, found 145.1107. $[\alpha]^{23}_D$ +2.1° (*c* 0.13, $CHCl_3$).

(*R*)-2-(Hydroxymethyl)-2,4,4-trimethylmorpholinium Iodide, (*R*)-2. To a solution of (*R*)-**12** (0.15 g, 1.0 mmol) in dry CH_3NO_2 (2 mL) was added CH_3I (0.29 g, 2.0 mmol). The flask was kept under dark for 5 h at room temperature. The solution was decanted, and the precipitate was washed with dry Et_2O (3 × 5 mL). The pale yellow solid was dried under vacuum to give 0.25 g (84%). The crude product was recrystallized initially from acetone followed by two recrystallizations from MeOH−Et_2O, which resulted in a constant optical rotation. Colorless crystals for X-ray analysis were obtained from MeOH by vapor diffusion with Et_2O. Mp: 155.3−155.8 °C. ^{1}H NMR (400 MHz, CD_3OD, TMS): 1.42 (s, 3H), 3.34 (s, 3H), 3.40 (s, 3H), 3.44−3.53 (m, 6H), 4.11−4.17 (m, 1H), 4.18−4.23 (m, 1H). ^{13}C NMR (100 MHz, CD_3OD, TMS): 20.4, 52.1, 55.4, 55.5, 59.9, 64.1, 66.6, 72.6. IR (KBr): 3346. MS (FAB): 164 ($M - I^-$). Anal. Calcd for $C_8H_{18}NO_2I$: C, 33.45; H, 6.32; N, 4.88. Found: C, 33.54; H, 6.31; N, 4.81. $[\alpha]^{23}_D$ +3.2° (*c* 0.8, MeOH).

Data for (*S*)-2: found C, 33.44; H, 6.28; N, 4.76. $[\alpha]^{23}_D$ − 3.2° (*c* 2.8, MeOH).

(*R*)-2,4-Dimethyl-2-[[(4-nitrophenyl)sulfonoxy]methyl]-morpholine, (*R*)-14. To a solution of (*R*)-**12** (0.40 g, 3.0 mmol) and NEt_3 (0.84 g, 8.3 mmol) in dry CH_2Cl_2 (15 mL) at room temperature was added 4-nitrobenzenesulfonyl chloride (0.67 g, 3.0 mmol) in dry CH_2Cl_2 (10 mL) dropwise in 30 min. The reaction mixture was stirred for 8 h and then washed with saturated $NaHCO_3$ (2 × 20 mL) and brine (1 × 25 mL). The solution was dried and concentrated to afford a dark red-brown oil, which was chromatographed on neutral alumina eluting with 10% EtOAc in hexanes to afford (*R*)-**14** as a yellow oil, which solidified overnight (0.60 g, 70%). Recrystallization from CH_2Cl_2−hexanes gave (*R*)-**14** as pale yellow needles. Mp: 187.9−188.6 °C dec. TLC R_f = 0.2 (5:1 hexanes−EtOAc, neutral alumina). ^{1}H NMR (400 MHz): 1.20 (s, 3H), 2.08 (d, J_{app} = 11.6 Hz, 1H), 2.16 (s, 3H), 2.20−2.25 (m, 2H), 2.32 (d, J_{app} = 11.6 Hz, 1H), 3.55−3.60 (m, 1H), 3.62−3.67 (m, 1H), 4.10 (d, J_{app} = 10 Hz, 1H), 4.30 (d, J_{app} = 10 Hz, 1H), 8.13 (d, J_{app} = 9.2 Hz, 2H), 8.41 (d, J_{app} = 9.2 Hz, 2H). ^{13}C NMR (100 MHz): 21.2, 46.3, 54.7, 60.7, 61.5, 71.7, 72.8, 124.3, 129.3, 141.8, 150.7. IR (neat): 1486. MS *m*/*z* (EI): 330 (M^+). Anal. Calcd for $C_{13}H_{18}N_2O_6S$: C, 47.26; H, 5.50; N, 8.48. Found: C, 46.99; H, 5.54; N, 8.45. $[\alpha]^{23}_D$ −11.5° (*c* 5.6, $CHCl_3$).

Data for (*S*)-14: found C, 47.19; H, 5.44; N, 8.40. $[\alpha]^{23}_D$ +11.3° (*c* 1.2, $CHCl_3$).

(*R*)-2,4,4-Trimethyl-2-[[(4-nitrophenyl)sulfonoxy]methyl]morpholinium Iodide, (*R*)-3. To a solution of (*R*)-**14** (0.090 g, 0.30 mmol) in dry CH_3NO_2 (1 mL) was added CH_3I (0.12 g, 0.82 mmol). The mixture was stirred for 36 h at room temperature. The solution was evaporated to dryness, and the residue was washed with dry Et_2O (3 × 5 mL). The pale yellow solid was recrystallized twice from acetone and Et_2O (0.12 g, 92%). Mp: 155.9−156.3 °C. ^{1}H NMR (400 MHz, CD_3OD, TMS): 1.41 (s, 3H), 3.27 (s, 3H), 3.33 (s, 3H), 3.35−3.50 (m, 4H), 3.90−3.97 (m, 1H), 4.05−4.12 (m, 1H), 4.21 (d, J_{app} = 10 Hz, 1H), 4.24 (d, J_{app} = 10 Hz, 1H), 8.20 (d, J_{app} = 9.2 Hz, 2H), 8.51 (d, J_{app} = 9.2 Hz, 2H). ^{13}C NMR (100 MHz, CD_3OD, TMS): 21.3, 53.5, 53.6, 56.9, 61.0, 64.7, 72.4, 74.6, 125.8, 128.0, 130.9, 142.7. IR (KBr): 1512. Anal. Calcd for $C_{14}H_{21}N_2O_6SI$: C, 35.59, H, 4.48, N, 5.93. Found: C, 35.65; H, 4.59; N, 6.05. $[\alpha]^{23}_D$ −12.9° (*c* 0.25, MeOH).

For (*S*)-3: found C, 35.61; H, 4.66; N, 6.11. $[\alpha]^{23}_D$ +12.7° (*c* 0.13, MeOH).

(*R*)-2-(Azidomethyl)-2,4-dimethylmorpholine, (*R*)-15. A solution of (*R*)-**14** (0.40 g, 1.0 mmol) and NaN_3 (3.4 g, 52 mmol) in DMF (5 mL) and water (1 mL) was heated at 70 °C for 72 h. The reaction mixture was poured in water (30 mL) and extracted into Et_2O (3 × 15 mL). The ethereal extract was washed with saturated $NaHCO_3$ (2 × 20 mL) and brine (1 × 25 mL). The extract was dried and concentrated to afford a yellow oil. The crude product was purified by chromatography on neutral alumina eluting with 5% EtOAc in hexanes to afford (*R*)-**15** as a colorless volatile liquid (0.13 g, 65%). TLC R_f = 0.3 (5:1 hexanes−EtOAc, neutral alumina). ^{1}H NMR (400 MHz): 1.26 (s, 3H), 2.13 (d, J_{app} = 11.2 Hz, 1H), 2.22 (s, 3H), 2.31−2.40 (m, 2H), 2.34 (d, J_{app} = 11.2 Hz, 1H), 3.25 (d, J_{app} = 12.8 Hz, 1H), 3.53 (d, J_{app} = 12.8 Hz, 1H), 3.77 (dd, J_{app} = 5.2, 4.8 Hz, 2H). ^{13}C NMR (100 MHz): 21.7, 46.5, 54.9, 55.9, 61.5, 61.6, 73.4. IR

(neat): 2107. MS *m*/*z* (EI): 170 (M^+). HRMS (CI): calcd for $C_7H_{15}ON_4$ 171.1247, found 171.1245. $[\alpha]^{23}_D$ −0.8° (*c* 0.48, $CHCl_3$).

For (*S*)-15: HRMS (CI) calcd for $C_7H_{15}ON_4$ 171.1247, found 171.1249. $[\alpha]^{23}_D$ +0.7° (*c* 0.26, $CHCl_3$).

(*R*)-2-(Azidomethyl)-2,4,4-trimethylmorpholinium Iodide, **(*R*)-4.** To a solution of (*R*)-**15** (0.050 g, 0.3 mmol) in dry CH_3NO_2 (1 mL) was added CH_3I (0.12 g, 0.87 mmol). The mixture was stirred for 24 h at room temperature. The solution was evaporated to dryness, and the residue was washed with dry Et_2O (3 × 5 mL). The pale white solid was recrystallized four times from MeOH and Et_2O to yield colorless, shiny plates (0.080 g, 90%). Mp: 128.2−128.7 °C. ^{1}H NMR (400 MHz, CD_3OD, TMS): 1.48 (s, 3H), 3.33 (s, 3H), 3.38 (s, 3H), 3.41−3.58 (m, 6H), 4.07−4.18 (m, 1H), 4.19−4.21 (m, 1H). ^{13}C NMR (100 MHz, CD_3OD, TMS): 22.1, 53.4, 56.9, 57.1, 58.7, 61.3, 65.7, 74.2. IR (KBr): 2116. MS (FAB): 164 ($M - I^-$). Anal. Calcd for $C_8H_{17}N_4OI$: C, 30.76; H, 5.49; N, 17.95. Found: C, 30.89; H, 5.56; N, 17.90. $[\alpha]^{23}_D$ −4.1° (*c* 2.8, MeOH).

For (*S*)-4: found C, 30.88; H, 5.53; N, 17.84. $[\alpha]^{23}_D$ +3.8° (*c* 3.4, MeOH).

[3-[(4-Nitrophenyl)sulfonoxy]phenyl]-*N,N,N*-trimethylammonium Iodide, **5.** To a solution of 3-(dimethylamino)-phenol (2.21 g, 15.8 mmol), DMAP (0.02 g), and NEt_3 (3.22 g, 31.6 mmol) in dry CH_2Cl_2 (10 mL) at room temperature was added 4-nitrobenzenesulfonyl chloride (3.71 g, 16.6 mmol) in dry CH_2Cl_2 (10 mL) dropwise in 30 min. The reaction mixture was stirred for 8 h and then washed with saturated $NaHCO_3$ (1 × 20 mL) and brine (1 × 25 mL). The solution was dried and concentrated to afford a dark red-brown oil, which was chromatographed on silica gel eluting with CH_2Cl_2 to afford a red oil, which solidified overnight. TLC R_f = 0.2 (CH_2Cl_2, silica). Recrystallization from acetone−ether gave reddish brown needles (4.8 g, 93%), which were converted into **5** by using a similar procedure to that described for the synthesis of **3**. Mp: 171.1−171.8 °C dec (acetone−Et_2O). ^{1}H NMR (400 MHz, CD_3OD): 3.7 (s, 9H), 7.35 (dd, J_{app} = 10, 2 Hz, 1H), 7.69 (t, J_{app} = 8.4 Hz, 1H), 7.86 (dd, J_{app} = 2.4, 2 Hz, 1H), 7.97 (dd, J_{app} = 8, 2.4 Hz, 1H), 8.18 (d, J_{app} = 9.2 Hz, 2H), 8.47 (d, J_{app} = 9.2 Hz, 2H). ^{13}C NMR (100 MHz, CD_3OD) 57.8, 116.9, 120.7, 125.7, 125.9, 131.5, 133.2. IR (KBr): 1505, 1434. Anal. Calcd for $C_{15}H_{17}N_2O_5SI$: C, 38.79; H, 3.69; N, 6.04. Found: C, 38.65; H, 3.74; N, 5.88.

Determination of Optical Purities of (*R*)- and (*S*)-12. A solution of morpholine alcohol **12** (0.050 g, 0.30 mmol) in dry EtOAc (1 mL) was added to a stirred mixture of (*R*)-(+)-MTPA (0.070 g, 0.30 mmol), DCC (0.070 g, 0.30 mmol), and DMAP (0.005 g, 0.5 mmol) in EtOAc (2 mL) under nitrogen. The mixture was stirred for 2 h at room temperature and then filtered to remove the precipitate. The precipitate was washed with EtOAc (2 × 5 mL). The filtrate was concentrated to give a pale yellow solid, which was purified by alumina preparative TLC eluting with 20% EtOAc−hexanes, collecting a wide UV active band to yield Mosher's ester **13**. The optical purities were determined by the average of integration of the signals for C-2 methyl, *N*-methyl, and CH_2OMTPA. TLC R_f = 0.25 (5:1 hexanes−EtOAc, neutral alumina). Mosher ester of (*R*)-**12**, ^{1}H NMR (400 MHz): 1.21 (s, 3H), 2.07 (d, J_{app} = 11.2 Hz, 1H), 2.18 (s, 3H), 2.31−2.40 (m, 2H), 2.37 (d, J_{app} = 11.2 Hz, 1H), 3.58 (s, 3H), 3.65−3.75 (m, 1H), 3.80−3.87 (m, 1H), 4.27 (d, J_{app} = 12.8 Hz, 1H), 4.59 (d, J_{app} = 12.8 Hz, 1H), 7.35−7.68 (m, 5H). Mosher ester of (*S*)-**12**, ^{1}H NMR (400 MHz): 1.18 (s, 3H), 2.07 (d, J_{app} = 11.2 Hz, 1H), 2.20 (s, 3H), 2.31−2.40 (m, 2H), 2.37 (d, J_{app} = 11.2 Hz, 1H), 3.56 (s, 3H), 3.68−3.74 (m, 1H), 3.79−3.85 (m, 1H), 4.35 (d, J_{app} = 12.8 Hz, 1H), 4.48 (d, J_{app} = 12.8 Hz, 1H), 7.35−7.68 (m, 5H). The ee values for (*R*) and (*S*)-**12** were 89.0 ± 0.4% and 91.5 ± 0.3%, respectively.

X-ray Experimental. X-ray diffraction data for both enantiomers were collected on an Enraf-Nonius CAD4 diffractometer equipped with Mo Kα radiation and a graphite monochromator. Two octants of data were collected for each. Data reduction included corrections for background, Lorentz polarization, and absorption effects. Absorption corrections were based on ψ scans. Refinement was done by full-matrix least-squares, with neutral-atom scattering factors and anomalous dispersion corrections. All non-hydrogen atoms were refined anisotropically. For both structures, the OH hydrogen atom was refined isotropically, while the other H atoms were placed in calculated positions. For (*S*)-**2**, R = 0.035, R_w = 0.039 for 2976 observations; for (*R*)-**2**, R = 0.034, R_w = 0.036 for 3214 observations. Refinement with reversed absolute configurations yielded R = 0.037, R_w = 0.041 for the *S* isomer and R = 0.038, R_w = 0.043 for the *R* isomer; thus both absolute configurations were proven.

Molecular Modeling. PCMODEL (version 4.0) (*17*) calculations with the default dielectric (1.5) and dielectric = 80 were performed on 72 unique conformations of **2**. These conformations included the nine possible staggered conformations for O−C−CH_2−O−H for chair and three unique twist−boat conformations of the ring. Axial and equatorial positions for hydroxymethyl were included for all ring conformations.

Molecular modeling studies (*18*) on (*R*)- and (*S*)-**2**−AChE complexes were done by placing (*R*)- and (*S*)-**2** in the same position as edrophonium (**19**) in the crystal structure of the **19**−AChE complex and then minimizing the whole structure.

Enzymatic Assays. (A) Materials. Sodium phosphate buffer components were reagent grade and used without further purification. Reactions were run in 0.08 M sodium phosphate buffer at pH 7.21. Grade V-S AChE (EC 3.1.1.7) from *Electrophorus electricus* was obtained as a lyophilized powder from Sigma Chemical Co. (St. Louis, MO), and prior to use the enzyme was dissolved in the phosphate buffer that contained 0.1 N NaCl. Acetylthiocholine chloride and 5,5′-dithiobis(2-nitrobenzoic acid) (DTNB) were also obtained from Sigma Chemical Co. and used as received.

(B) Kinetic Measurements. AChE activity was measured at 25.0 ± 0.1EC by the coupled assay method described by Ellman et al. (*19*). Time courses were followed at 412 nm and were fit to the integrated Michaelis−Menten equation to obtain values of K_m and V_{max}, as described by Lee et al. (*8*). The initial substrate concentration was 0.5 mM. Inhibition was characterized by running reactions in the absence of inhibitor (control) and in the presence of at least four fixed inhibitor concentrations. Controls and inhibition reactions were run at least in duplicate.

Scheme 1. Synthesis of Morpholine Alcohols

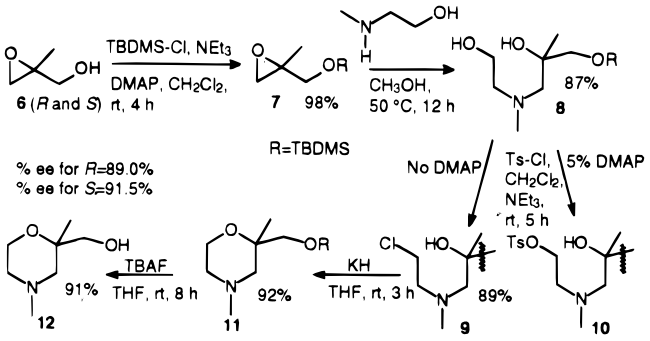

Results

Our synthesis (Scheme 1) started with commercially available (*R*)- and (*S*)-2-methylglycidols, **6**, having optical purity of about 90%. After protection of the hydroxyl group of **6** with TBDMS (*16*), the epoxides reacted with *N*-methyl-2-aminoethanol to give **8**. Amino diol **8** when treated with tosyl chloride and triethylamine gave the chloro compound **9** in a quantitative yield, instead of the expected primary tosylate **10**. Adding DMAP (*20*) to the reaction gave **10** exclusively. We presumed that in the absence of DMAP, chloride displaced tosylate via an S_N2 mechanism to give **9**. Treatment of **9** with potassium

Scheme 2. Synthesis of Quaternary Morpholinium Iodides

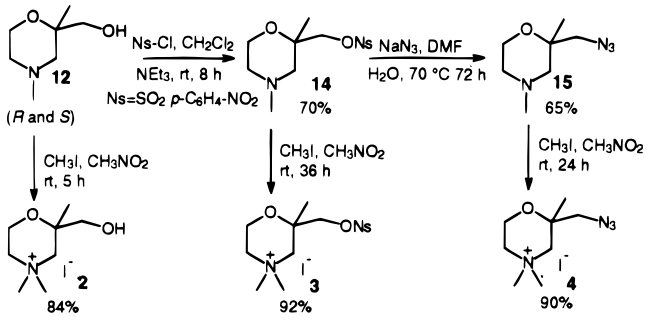

hydride in THF closed the ring to yield **11**. Removal of the TBDMS group of **11** furnished **12** in quantitative yield.

The optical purity of **12** was measured by converting it into a Mosher ester, **13** (not shown). Quaternarization of **12** gave **2**, which was recrystallized to give a sample with constant rotation and a sharp melting point. Single-crystal X-ray analysis confirmed the absolute configurations of both enantiomers of **2**.

Morpholinyl alcohol **12** was converted into nosylate **14** (Scheme 2). Quaternarization of **14** gave **3** in 92% yield. Treatment of **14** with 50-fold excess of sodium azide in DMF at 70 °C for 72 h gave the azidomorpholine **15** in a moderate yield. Nucleophilic displacement at this neopentyl center required a long reaction time. Compound **15** was subsequently quaternarized to the azidomorpholinium iodide **4**.

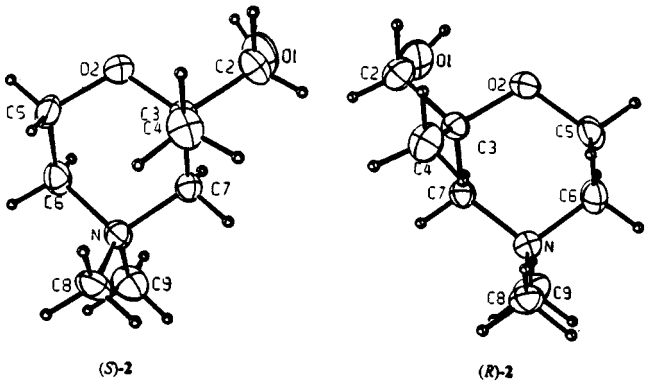

Figure 1. ORTEP drawings of (*S*)- and (*R*)-**2**.

Structure. 1. Crystal. In the crystal (Figure 1) the morpholinium ring adopts a chair conformation with the hydroxymethyl group in an equatorial position. The bond distances and angles for (*R*)- and (*S*)-**2** are similar to those of the carnitine analogues (*14*) **16** and **17**. The only

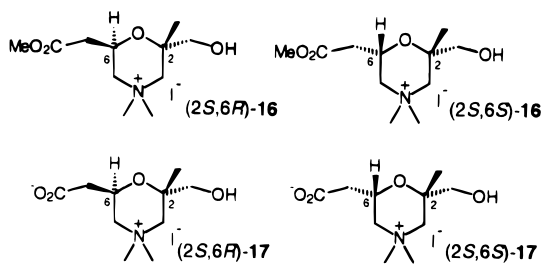

significant difference is in the torsion angle of the hydroxymethyl group. The O−C−CH_2−OH torsion angle is gauche, 62.8(4)° and −62.6(5)°, in (*R*)- and (*S*)-**2**, respectively. This torsion angle in (2*S*,6*S*)-**16** and (2*S*,6*S*)-**17** is also gauche, but it is anti in (2*S*,6*R*)-**16** and (2*S*,6*R*)-**17**. These differences are due to intermolecular hydrogen bonding. For (*S*)-**2**, there is a weak hydrogen bond between O1−H and an iodide with an O1−I distance of 3.747(4) Å.

2. Solution NMR. The similarity in chemical shifts (at 400 MHz) of the morpholinium ring protons at C-5 and C-3 has thwarted assignment of individual resonances. The axial and equatorial *N*-methyl groups show a chemical shift difference of approximately 0.05 ppm. Our attempts to assign them and the rest of the axial or equatorial protons in all three compounds using COSY, NOE difference, 2D-NOESY, ROESY, and HETCOR experiments have met with little success.

3. Molecular Mechanics. To understand how these inhibitors might bind to AChE, we need to analyze the preferred conformations. Using PCMODEL (*17*) at both the default dielectric and a dielectric = 80, we find that chair conformers predominate. Surprisingly, twist−boat conformations account for 14% of the total population. In the 86% of the population that are chair conformers, an equatorial hydroxymethyl group is preferred over an axial one (51:35). The calculated most stable conformation, which is only 24% of the population, is the same conformation observed in the solid state. The lack of reliable parameters for sulfonoxy and azido makes calculations on **3** and **4**, respectively, unfeasible at this time. We are studying the conformational properties of **2** with other computational methods to confirm and explain this unusually large percentage of twist−boat conformers.

Inhibition of AChE. 1. Competitive Inhibition. Compounds **2** and **4** are reversible competitive AChE inhibitors; that is, as inhibitor concentration [I] increases, K_m increases but V_{max} remains relatively constant. In this case V/K ($=V_{max}/K_m$) is a decreasing nonlinear function of increasing inhibitor concentration [I], as described in eq 1:

$$(V/K)_I = (V/K)_0 \frac{K_i}{K_i + [I]} \qquad (1)$$

$(V/K)_I$ and $(V/K)_0$ are V/K values in the presence and absence of inhibitor, and K_i is the dissociation constant of the reversible EI complex. The adjustable parameters $(V/K)_0$ and K_i were calculated by fitting data to eq 1 by nonlinear least-squares procedures. Figure 2 shows such a fit for inhibition of AChE by (*S*)-**2**. Compound (*S*)-**2** inhibits 1.8-fold more strongly than (*R*)-**2**, but **4** shows virtually no difference between the two enantiomers (Table 1).

2. Noncompetitive Inhibition. Compounds **3** and **5** show linear noncompetitive inhibition. The agreement between K_i calculated by fitting V/K versus [I] data to eq 1 and K_i' calculated by fitting V versus [I] data to eq 2:

$$V_i = \frac{V_0}{1 + \frac{[I]}{K_i}} \qquad (2)$$

provides an additional indication of linear noncompetitive inhibition. In this case, both V/K and V ($=V_{max}$) are decreasing nonlinear functions of increasing [I]. This type of inhibition occurs when the inhibitor binds at the

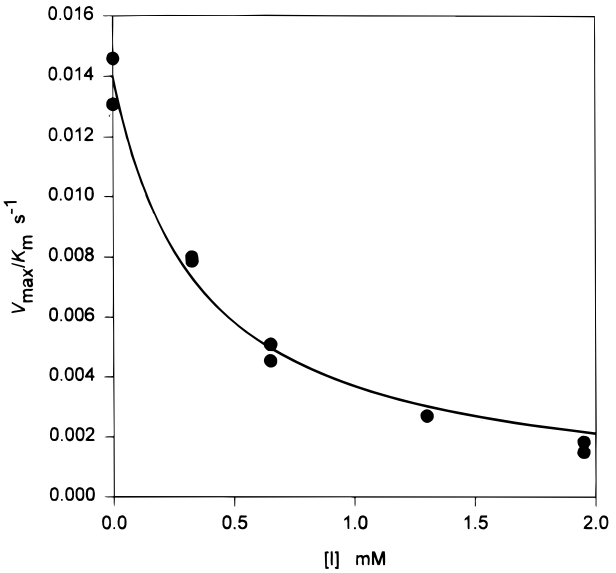

Figure 2. Fit of V/K versus inhibitor concentration of (*S*)-**2** to eq 1 (see text). The inhibition constant, K_i, calculated from nonlinear least-squares method, is 360 ± 30 μM.

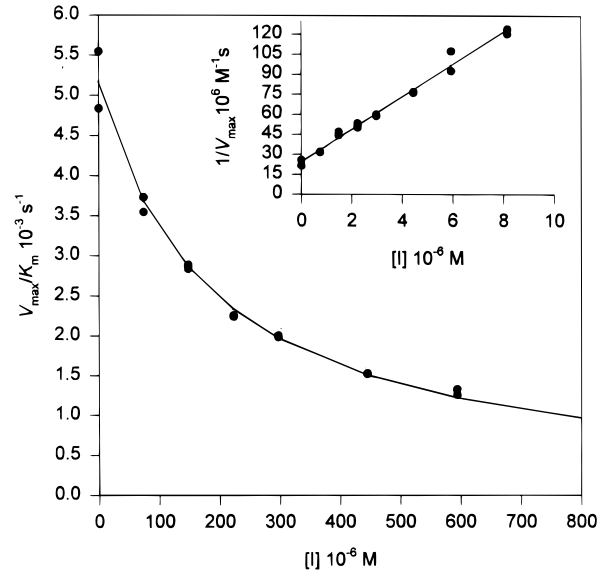

Figure 3. Fit of V/K versus inhibitor concentration of (*S*)-**3** to eq 1. The inhibition constant, K_i, calculated from nonlinear least-squares method, is 19.0 ± 0.9 μM. Inset: Plot of $1/V_{max}$ versus inhibitor concentration of (*S*)-**3** shows a linear noncompetitive inhibition.

Table 1. *E. electricus* AChE Inhibition by Morpholiniums at 25 ± 0.1 °C and pH 7.21

	K_i, μM	
inhibitor, mode	configuration at C-2: *S*	configuration at C-2: *R*
2, reversible competitive	360 ± 30	650 ± 90
3, noncompetitive	19.0 ± 0.9	50 ± 2
4, reversible competitive	450 ± 70	560 ± 30

peripheral site, does not compete with the substrate at the active site, and has no effect on K_m. Figure 3 shows a plot of V_{max}/K_m against [I], where I = (*S*)-**3**, and a plot (inset) of $1/V_{max}$ against [I], which indicates a linear noncompetitive inhibition. Both (*R*)- and (*S*)-**3** show linear noncompetitive inhibition; (*S*)-**3** is 2.5-fold more active than (*R*)-**3**. Compound **5** is 3-fold more active than (*S*)-**3**.

Table 2. Comparison of Inhibition of AChE

inhibitor	K_i, μM
1a, R = H, X = Cl	560 ± 50[a]
1b, R = CH_3, X = Br	550 ± 20[a]
1c, R = *p*-C_6H_4−NH_2, X = Br	220 ± 50[a]
1d, R = *p*-C_6H_4−NO_2, X = Br	1630 ± 70[a]
1e, R = *p*-C_6H_4−CN, X = Br	3690 ± 90[a]
(*S*)-**2**	360 ± 30[b]
(*S*)-**3**	19.0 ± 0.9[b]
18	0.21 ± 0.06[a]
5	6.0 ± 0.5[b]

[a] Reference 8. [b] This work.

Discussion

Strong stereoselectivity, our initial rationale for assaying **2**−**4**, does not occur. The lack of stereoselectivity for the azide **4** is especially disappointing and excludes further experiments with these analogues. Below, we discuss the modest stereoselectivity of **2**. The discovery in this study is the noncompetitive inhibition by **3** compared to the competitive inhibition by **2** and **4**. Furthermore, **3** is 10-fold more active than **2** or **4**. The noncompetitive inhibition by **5** supports the conclusion that the (4-nitrophenyl)sulfonoxyl group controls the mode of inhibition. Comparing these results with other inhibitors underscores this conclusion.

Comparison with Hemicholiniums. Both **2** and **4** have K_i values similar to those of the racemic alkyl hemicholiniums **1a**,**b** (Table 2). All aryl hemicholiniums, with **1c** as the best, show competitive inhibition. As **1c** is open and closed (*9*), AChE may stabilize one form over the other. If AChE stabilizes the closed form, comparison of **1c** with **3** suggests that changing OH and aryl to CH_3 and CH_2OSO_2-aryl, respectively, results in a change from competitive to noncompetitive inhibition. Furthermore, (*R*)- and (*S*)-**3** inhibit significantly better than aryl hemicholiniums, especially **1d**, where R = *p*-C_6H_4-NO_2. The comparison here, however, is not equivalent; **3** inhibits in the peripheral site, while **1d** inhibits in the active site. For competitive inhibition, electron-rich aryl hemicholinium groups inhibit better than electron-poor. Whether the reverse is true for noncompetitive inhibition by the arylsulfonoxyl group remains to be tested.

Comparison of Morpholiniums and Aryltrimethylammoniums. The strong AChE inhibitor (3-hydroxyphenyl)trimethylammonium iodide (**18**; Table 2), an analogue of edrophonium, **19**, has three carbon atoms between the $(CH_3)_3N^+$ and the OH as **2,** but **18** (K_i = 0.21 μM) (*8*) is over 1700-fold more potent than (*S*)-**2**. Compound **18** (pK_a = 8.2) should be a better hydrogen-bond donor than (*S*)-**2** (estimated $pK_a \sim 16$). The acceptor is an imidazolyl nitrogen (pK_a = 6.3) in the active site. The closer the match in pK_a between the donor and the acceptor, i.e., $\Delta pK_a \sim 0$, the stronger the hydrogen bond. The X-ray structure of the **19**−AChE complex shows that the quaternary nitrogen of **19** is positioned next to the indole ring of Trp84, while the *m*-hydroxyl group of **19** is positioned between His440 and Ser200, thus forming hydrogen bonds with two of the three members of the catalytic triad (*21*).

Our molecular modeling studies done by replacing **19** with (*R*)- and (*S*)-**2** in the **19**−AChE complex reveal that such a hydrogen bond is only possible with (*S*)-**2**, where the quaternary nitrogen could interact favorably with Trp84. This can explain the 1.8-fold stereochemical preference for (*S*)-**2**.

Substituting 4-nitrobenzenesulfonyl for hydrogen in (*S*)-**2** and **18** to give (*S*)-**3** and **5**, respectively, results in a change from competitive to noncompetitive inhibition.

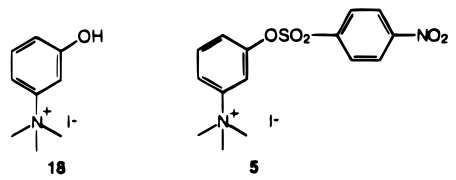

18 **5**

In addition, the 4-nitrobenzenesulfonyl group levels the potency of these two classes of AChE inhibitors. Inhibitor **5** is 3-fold more potent than (*S*)-**3**, which is a marked contrast to the 1700-fold enhancement of **18** compared to (*S*)-**2**. In the case of **5** compared to **18**, the K_i decreases 28-fold. Loss of the strong hydrogen bond between **18** and His440 reduces the potency. The 4-nitrobenzenesulfonyl group controls the mode of inhibition and apparently the affinity of (*S*)-**3** and **5** for AChE.

Why do **3** and **5** bind to the peripheral site and not the active site? (3-Hydroxyphenyl)trimethylammonium iodide and the methylsulfonoxy derivative, strong competitive inhibitors of AChE, have values of $K_i = 0.21$ (*8*) and 0.4 (*22*) μM, respectively. The 4-nitrophenyl hemicholinium **1d** is also a competitive inhibitor. Therefore, either a sulfonoxyl group or a 4-nitrophenyl group is not sufficient individually to change the mode of inhibition. The combination of both moieties appears as essential for changing the mode of inhibition. We do not know at this point whether any other arylsulfonoxyl derivatives of **3** and **5** will be noncompetitive inhibitors. No matter what the explanation, the change in the mode of inhibition provides a lead to design more analogues.

Summary

We have achieved a chiral, five-step synthesis of 2-(hydroxymethyl)-2,4-dimethylmorpholine from (*R*)- and (*S*)-2-methylglycidols in an overall yield of 63%. Morpholinium salts, **2**, **3**, and **4** inhibit AChE. Enantiomers of **2** and **4** are reversible competitive inhibitors of AChE, whereas enantiomers of **3** are noncompetitive inhibitors of AChE. A competitive AChE inhibitor (**18**) when converted into the 4-nitrobenzenesulfonyl derivative yields a noncompetitive inhibitor, **5**, but with reduced potency. In **2** and **3**, a small amount of chiral discrimination is seen. The inhibition results provide leads for elaborating the design to produce more potent chiral inhibitors. The successful strategy of connecting moieties that bind concurrently at both the active and the peripheral sites (*4*) will guide our future efforts.

Acknowledgment. R.D.G. thanks the National Institute of Health for support of this work through Grant GM42016. We thank the reviewers for their valuable comments and suggestions.

References

(1) Rosenberry, T. L. (1975) Acetylcholinesterase. *Adv. Enzymol. Relat. Areas Mol. Biol.* **43**, 103−218.

(2) Quinn, D. M. (1987) Acetylcholinesterase. Enzyme structure, reaction dynamics and virtual transition states. *Chem. Rev.* **87**, 955−979.

(3) Stedman, E. (1929) Studies on the relationship between chemical constitution and physiological action. Part II. The miotic activity of urethanes derived from the isomeric hydroxybenzyldimethylamines. *Biochem. J.* **23**, 17−24.

(4) Pang, Y.-P., Quiram, P., Jelacic, T., Hong, F., and Brimijoin, S. (1996) Highly potent, selective, and low-cost bis-tetrahydroaminacrine inhibitors of acetylcholinesterase: step toward novel drugs for Alzheimer's disease. *J. Biol. Chem.* **271**, 23646−23649.

(5) Sussman, J. L., Harel, M., Frowlow, F., Oefner, C., Goldman, A., Toker, L., and Silman, I. (1991) Atomic structure of acetylcholinesterase from *Torpedo californica*: a prototypic acetylcholine binding protein. *Science (Washington, D.C.)* **253**, 872−879.

(6) Haworth, R. D., Lamberton, A. H., and Woodcock, D. (1947) Investigations on the influence of chemical constitution upon toxicity. Part I. Compounds related to Doryl. *J. Chem. Soc.* 176−182.

(7) Harel, M., Schalk, I., Ehret-Sabatier, L., Bouet, F., Goeldner, M., Hirth, C., Axelsen, P. H., Silman, I., and Sussman, J. L. (1993) Quaternary ligand binding to aromatic residues in the active-site gorge of acetylcholinesterase. *Proc. Natl. Acad. Sci. U.S.A.* **90**, 9031−9035.

(8) Lee, B. H., Stelly, T. C., Colucci, W. J., Garcia, J. G., Gandour, R. D., and Quinn, D. M. (1992) Inhibition of acetylcholinesterase by hemicholiniums, conformationally constrained choline analogues. Evaluation of aryl and alkyl substituents. Comparison with choline and (3-hydroxyphenyl)trimethylammonium. *Chem. Res. Toxicol.* **5**, 411−418.

(9) Sørensen, P. E., McClelland, R. A., and Gandour, R. D. (1991) Intramolecular hemiacetals. The acid−base-catalyzed ring-chain interconversion of 2-substituted 2-hydroxy-4,4-dimethylmorpholinium cations in aqueous solution. *Acta Chem. Scand.* **45**, 558−566.

(10) Yanagisawa, H., and Kanazaki, T. (1993) Facile synthesis of optically active 4-*tert*-butoxycarbonyl-2-hydroxymethylmorpholine. *Heterocycles* **35**, 105−109.

(11) Morie, T., Kato, S., Harada, H., Yoshida, N., and Matsumoto, J. (1994) Synthesis and biological activities of the optical isomers of (±)-4-amino-5-chloro-2-ethoxy-*N*-[[4-(4-fluorobenzyl)-2-morpholinyl]methyl]benzamide (Mosapride). *Chem. Pharm. Bull.* **42**, 877−882.

(12) Licandro, E., Maiorana, S., Papagni, A., Pryce, M., Gerosa, A. Z., and Riva, S. (1995) Asymmetric synthesis of (−)-(2*R*,6*R*)-2,6-dimethylmorpholine. *Tetrahedron: Asymmetry* **6**, 1891−1894.

(13) Thorey, C., Wilken, J., Hénin, F., Martens, J., Mehler, T., and Muzart, J. (1995) Diastereoselective synthesis of vinylmorpholines by palladium-catalyzed tandem allylic substitutions using enantiopure amino alcohols as bifunctional nucleophiles. *Tetrahedron Lett.* **36**, 5527−5530.

(14) Sun, G., Savle, P. S., Gandour, R. D., Nic a' Bhaírd, N., Ramsay, R. R., and Fronczek, F. R. (1995) Syntheses, structures, and enzymatic evaluations of conformationally constrained, analogue inhibitors of carnitine acetyltransferase: (2*R*,6*R*)-, (2*S*,6*S*)-, (2*R*,6*S*)-, and (2*S*,6*R*)-6-carboxylatomethyl-2-hydroxymethyl-2,4,4-trimethylmorpholinium. *J. Org. Chem.* **60**, 6688−6695.

(15) Blythin, D. J., Kuo, S.-C., Shue, H.-J., McPhail, A. T., Chapman, R. W., Kreutner, W., Rizzo, C., She, H. S., and West, R. (1996) Substituted morpholine-2*S*-acetic acid derivatives: Sch 50911 and related compounds as novel $GABA_B$ antagonists. *Bioorg. Med. Chem. Lett.* **6**, 1529−1534.

(16) Wipf, P., and Xu, W. (1993) Organozirconocenes in organic synthesis: tandem epoxide rearrangement-carbonyl addition. *J. Org. Chem.* **58**, 825−826.

(17) Gajewski, J. J., and Gilbert, K. E. (1992) *PCMODEL Molecular Modeling Package*, version 4.0, Serena Software, P.O. Box 3076, Bloomington, IN 47402.

(18) *SYBYL Molecular Modeling Package*, version 6.1 (1994) Tripos, Inc., St. Louis, MO 63144.

(19) Ellman, G. L., Coutney, K. D., Andres, V., Jr., and Featherstone, R. M. (1961) A new and rapid colorimetric determination of acetylcholinesterase activity. *Biochem. Pharmacol.* **7**, 88−95.

(20) Lee, J. H., Cho, Y. H., Lee, H. K., and Cho, S. H. (1995) A facile one-pot transformation of carboxylic acids to amides. *Synth. Commun.* **25**, 2877−2881.

(21) Sussman, J. L., Harel, M., and Silman, I. (1993) Three-dimensional structure of acetylcholinesterase and of its complexes with anticholinesterase drugs. *Chem. Biol. Interact.* **87**, 187−197.

(22) Kitz, R., and Wilson, I. B. (1962) Esters of methanesulfonic acid as irreversible inhibitors of acetylcholinesterase. *J. Biol. Chem.* **237**, 3245−3249.

TX970019O